Eawag
Swiss Federal Institute of Aquatic Science and Technology

Spike
Sensor management, Process Intelligence and Control at Eawag

Technical Report No. 1, v1.1

(TR-001-01-1)

Bounding Procedures for Shape Constrained Splines with Discontinuities

Author:
Kris Villez

Dübendorf, Switzerland
Originally published: 12/11/2014
Last update: 19/08/2015

K. Villez (2014). *Bounding Procedures for Shape Constrained Splines with Discontinuities.* Eawag, Dübendorf, Switzerland, Technical Report TR-001-01-1.

Abstract

Previous work on qualitative trend analysis (QTA) has led to the development of a shape constrained splines (SCS) method. This method delivers a deterministic and globally optimal solution for the location of so called transitions in a qualitative representation (QR). Unfortunately, this method is limited in the sense that discontinuities of one or more derivatives of the fitted function imposed by shape constraints on otherwise continuous derivatives are not permitted. Indeed, the bounding procedures available so far for deterministic global optimization by means of the branch-and-bound algorithm are limited to this case. This technical report discusses the necessary modifications to the SCS method which are necessary to permit the globally optimal identification of transitions with shape constrained splines with discontinuities (SCSD).

1 Introduction

Qualitative trend analysis (QTA) represents a set of algorithms inspired by ideas based in artificial intelligence and data mining. Most typically, these methods are applied in contexts where both precise knowledge and voluminous data sets are lacking, e.g., fault detection and identification [1]. Following negative results obtain by benchmarking [2], a new method based on shape constrained splines (SCS) has been proposed in [3]. Unfortunately, this method exhibits a number of inherent limitations which are extensively discussed in [3]. One of these limitations is that the fitted spline functions are necessarily continuous for all derivatives until the d^{th} derivative, with d the degree of the spline function (order: $d + 1$). This implies that certain qualitative sequences (QSs, definition below) cannot be applied. An example is given below.

The main purpose of this document is to describe the necessary modifications to the SCS method which enable application of QSs implying the presence of multiple knots in a single argument. The branch-and-bounding algorithm is applied without modification. The bounding procedures are different however. This report is therefore focused on the computation of the lower and upper bounds to the objective function. A didactic example is used to demonstrate the obtained results.

This section continues with necessary definitions (Section 1.1) and an introduction of the example (Section 1.2). Thereafter, Section 2 discusses the mathematical formulation of the shape constrained spline function fitting problem. Section 3 discusses the solution to this problem if the transitions (definition below) are known. Section 4 discusses the required bounding procedures to solve for the a priori unknown transitions. Summary conclusions are given in Section 6.

1.1 Definitions and notation

The following definitions are used in this work:

Episode. An episode is an argument interval over which the signs of a function or data series and/or one or more of its derivatives does not change. It is defined by a primitive, a start time, and an end time.

Primitive. A primitive is a unique combination of signs for a value of a function and/or one or more of its derivatives. Each primitive is usually referred to by means of an arbitrary chosen character. In this work, the sign of the first and second derivatives of a quadratic spline function are of interest. The correspondence between the signs of the derivatives and the characters used in this study are given in Fig. 1.

Qualitative sequence. A qualitative sequence (QS) is a series of primitives. Such a QS is used to describe the assessed or expected shape of a function or time series. A QS does not include the argument locations (transitions) at which a change in primitive is expected or observed.

Transition. A transition is defined as the argument location of a change-point between two sequential primitives.

Qualitative representation. A qualitative representation is a complete description of the expected or observed shape of a function or time series and consists of a QS and values for the argument values of the corresponding transitions.

A qualitative sequence is defined mathematically by means of integers, $s_{e,j}$, with e indicating the index of the primitive in the QS ($e = 0 \dots n_e$) and j indicating the considered derivative ($j \geq 0$). The transitions between primitives are given as a vector $\boldsymbol{\theta} = \left[\begin{array}{cccc} \theta_1 & \theta_2 & \dots & \theta_{n_e} \end{array}\right]$. A number of transitions are considered to imply a discontinuity in one or more derivatives which are

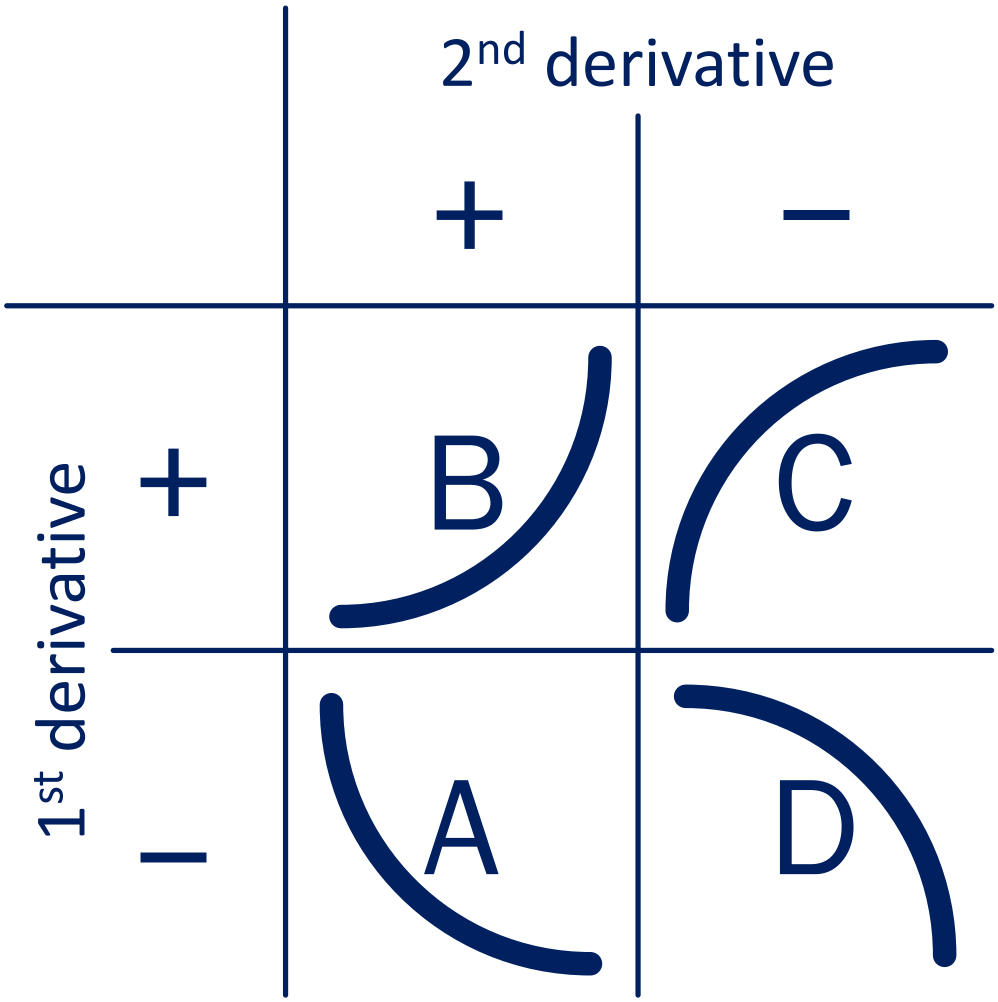

Figure 1: Primitives according to the signs of the 1st and 2nd derivative: A = anti-tonic convex, B = isotonic convex, C = isotonic concave, D = anti-tonic concave. Taken from [Villez2014]

otherwise piece-wise continuous. These are given as $\boldsymbol{\delta} = \left[\begin{array}{cccc} \delta_1 & \delta_2 & ... & \delta_{n_d} \end{array} \right]$ and are a subset of θ:

$$\boldsymbol{\delta} \subseteq \boldsymbol{\theta} \tag{1}$$

1.2 Example

The obtained results are demonstrated by means of a simple simulated batch experiment with a first-order Single-Input-Single-Output (SISO) process. The first order process dynamics are written in the time domain as follows:

$$dy/dx \quad = \quad \frac{1}{\tau} \cdot y(x) + u(x) \tag{2}$$

The response is simulated with $\tau = 3$, $y(0) = 0$ and from $t = 0$ until $t = 16$ and with inputs as follows:

$$u(x) \quad = \quad \begin{cases} 1, & \mathit{if}\; 0 \leq x \leq \theta \\ 0, & \mathit{otherwise} \end{cases} \tag{3}$$

The value of θ is simulated to be 7.5 Analytically, the process response is written as follows:

$$y(x) \quad = \quad (1 - e^{-\frac{x}{\tau}}) - H(x-\theta) \cdot (1 - e^{-\frac{x-\theta}{\tau}}) \tag{4}$$

with H the Heaviside step function. Simulated noise-free measurements are obtained by sampling the process at every unit interval ($t = 0, 1, 2, ..., 16$). Fig. 2 displays the simulated process state and measurements.

The simulated profile has a CA shape (cfr. definitions in [1]). Indeed, one can clearly identify that a first episode, with positive 1$^{\text{st}}$ derivative and negative 2$^{\text{nd}}$ derivative, is followed by a second episode, with negative 1$^{\text{st}}$ derivative and positive 2$^{\text{nd}}$ derivative. As such, this qualitative sequence implies a discontinuity in the first and second derivatives between these two episodes. Identifying the location of the transition between these episodes is impossible with the original SCS method [1]. Thanks to the generalized modified procedures below for shape constrained splines with discontinuities (SCSD), this is now possible.

2 Problem formulation

2.1 General formulation for any function

Consider that a sequence of n data pairs, (x_i, y_i), is given as a vector of arguments, $\boldsymbol{x} = \{x_1, x_2, ...x_i, ..., x_n\}$ and a matching vector of measurement

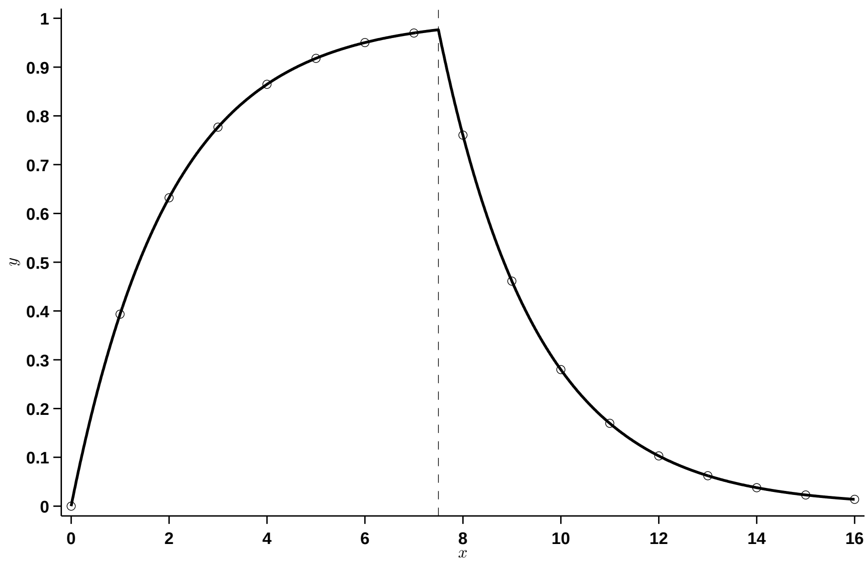

Figure 2: Simulated example.

values, $\boldsymbol{y} = \{y_1, y_2, ..., y_i, ..., y_n\}$. Then, the problem of fitting a shape constrained function can be written in a very general form as follows:

$$\min_{\boldsymbol{\beta},\boldsymbol{\theta}} g(\boldsymbol{\beta}) \quad = \quad g(\boldsymbol{\beta}, \boldsymbol{x}, \boldsymbol{y}) \tag{5}$$

subject to:

$$\boldsymbol{\beta} \quad \in \quad \Omega(\boldsymbol{\theta}) \tag{6}$$

$$\boldsymbol{\theta} \quad \in \quad \Theta \tag{7}$$

and with definitions as follows:

$\boldsymbol{\beta}$	Parameters of the unconstrained function
$\boldsymbol{\theta}$	Transitions defining the enforced shape of the function
$\boldsymbol{x}$	Data point arguments
$\boldsymbol{y}$	Data point measurements
g	Objective function
$\Omega(\boldsymbol{\theta})$	Feasible set for $\boldsymbol{\beta}$, which depends on $\boldsymbol{\theta}$
Θ	Feasible set for $\boldsymbol{\theta}$

The global solution to the above problem can be solved deterministically when the following holds (sufficient conditions):

1. The set $\Omega(\boldsymbol{\theta})$ is convex for any given $\boldsymbol{\theta}$.
2. The objective function g is convex in the parameters $\boldsymbol{\beta}$.
3. Bounds to the objective function g can be computed for any feasible subset of Θ.

2.2 Specific formulation for spline functions

To obtain provable bounds, the fitted function is restricted to the family of spline functions. Furthermore, the objective function consists of a penalty on the fit, defined as a norm on the residuals, and additional ridge-like second-order penalties for one or more derivatives of the fitted function. The applied set of knots consist of a set of n_{fix} knot locations, $\boldsymbol{\kappa}_{fix}$, with fixed argument values and a set of n_{var} knot locations, $\boldsymbol{\kappa}_{var}$, with variable argument values. The latter set of knots corresponds to the subset of the transitions in the considered Qualitative Sequence (QS) which imply a discontinuity in the fitted function and/or one or more of its derivatives, given above as $\boldsymbol{\delta}$ ($\boldsymbol{\delta} = \boldsymbol{\kappa}_{var}$). Naturally, the number of variable knot locations, n_{var}, is equal to the number of transitions in the QS implying a discontinuity, n_d.

With the complete set of transition arguments written as follows:

$$\boldsymbol{\theta} = \left[\begin{array}{cccc} \theta_1 & \theta_2 & \dots & \theta_{n_e} \end{array} \right] \tag{8}$$

it holds for the variable knot arguments that:

$$\boldsymbol{\kappa}_{var} = \boldsymbol{\delta} \subseteq \boldsymbol{\theta} \tag{9}$$

It is ensured that the set of fixed knots and variable knots is always mutually exclusive so that:

$$\boldsymbol{\kappa}_{fix} \cap \boldsymbol{\kappa}_{var} = \boldsymbol{\kappa}_{fix} \cap \boldsymbol{\delta} = \varnothing \tag{10}$$

The union of applied knots is given as:

$$\boldsymbol{\kappa} = \boldsymbol{\kappa}_{fix} \cup \boldsymbol{\kappa}_{var} = \boldsymbol{\kappa}_{fix} \cup \boldsymbol{\delta} \tag{11}$$

and consists of a total of n_a knots with argument values a_k ($k = 1 \dots n_a$).

A degree of continuity, c_k, is associated with each knot in $\boldsymbol{\kappa}$ and specifies the highest derivative which is continuous in the considered knot. The degree of continuity for the k^{th} variable knot location is given as $c_{var,k}$. In a spline without any discontinuities, this integer is equal to d (spline polynomial degree). The bounding procedures that follow however allow to apply lower integers, thus allowing discontinuous behaviour for one or more derivatives in both fixed and variable knot locations.

With the above specifications, the shape constrained spline fitting problem can be written as follows:

$$\min_{\boldsymbol{\beta},\boldsymbol{\theta}} g(\boldsymbol{\beta}) \quad = \quad |\boldsymbol{y} - f(\boldsymbol{\beta},\boldsymbol{x})|^p + \sum_{j=0}^{j=d} \lambda_j \cdot \int_{x_1}^{x_n} |f^j(\boldsymbol{\beta},v)|^{q_j} \; dv \tag{12}$$

subject to:

$$\forall k = 1 \dots n_a, \forall j = 0 \dots c_k \quad : \quad \lim_{v \to a_k^-} f^j(\boldsymbol{\beta},v) = \lim_{v \to a_k^+} f^j(\boldsymbol{\beta},v) \tag{13}$$

$$\forall e = 0 \dots n_e, \forall j = 0 \dots d :$$

$$b_e^L \leq v \leq b_e^U \quad \Rightarrow \quad \begin{cases} f^j(\boldsymbol{\beta},v) \leq 0, & \textit{if } s_{e,j} = -1 \\ f^j(\boldsymbol{\beta},v) = 0, & \textit{if } s_{e,j} = 0 \\ f^j(\boldsymbol{\beta},v) \geq 0, & \textit{if } s_{e,j} = +1 \end{cases} \tag{14}$$

$$\boldsymbol{b}^L = [\ b_0^L \quad b_1^L \quad \dots \quad b_{n_e}^L\ ] \quad = \quad [\ x_1 \quad \theta_1 \quad \theta_2 \quad \dots \quad \theta_{n_e}\ ] \tag{15}$$

$$\boldsymbol{b}^U = [\ b_0^U \quad b_{U,1} \quad \dots \quad b_{n_e}^U\ ] \quad = \quad [\ \theta_1 \quad \theta_2 \quad \dots \quad \theta_{n_e} \quad x_n\ ] \tag{16}$$

with:

$\boldsymbol{a}$	Internal knots of the spline function
$\boldsymbol{b}$	Boundary argument values for each episode
c	Integers indicating the highest derivative with retained continuity
d	Degree of the polynomials
j	Derivative index
k	Internal knot index

3 Solving for β

3.1 Strategy

When the values for θ are known, the complete qualitative representation (QR) is specified. Following the work of [4, 5], the above problem is reduced to a convex optimization problem. Depending on the order of the piece-wise polynomials and the applied constraints on the derivatives, the set $\Omega(\boldsymbol{\theta})$ is described by a combination of linear equalities and/or inequalities, second-order cone inequalities, and/or semi-definite cone inequalities as constraints. In all cases, this set remains convex as does the objective function. As a result, interior-point algorithms can be used to efficiently solve this problem. Specialized packages such as CVX include such interior-point algorithms [6]. Without loss of generality, the problems studied here exclude semi-definite cones as constraints. This permits the use of software specialized to solve second order cone programs (SOCP) such as Mosek which is generally faster than the more general interior-point optimizers [7, 8]. Practically this means that the application of inequality constraints is limited to derivatives of the fitted spline function which can be written as piece-wise polynomials of order 4 (cubic) or lower.

3.2 Demonstration

The top panel of Fig. 3 displays the fit of two quadratic (3^{rd} order) spline functions to the example introduced above. The spline functions are characterized by (i) nine (9) fixed knots with multiplicity in the arguments 0 until 16 in steps of two and (ii) one fixed knot with multiplicity of two (2) in the argument 7.5. The first of these functions is fitted without any constraints. The second is constrained with an imposed CA shape with its transition argument coinciding with the knot with multiplicity. One observes a relatively good fit for this function. Interestingly, the shape constraint reduces the deviations between the simulated function and the fitted function (bottom panel).

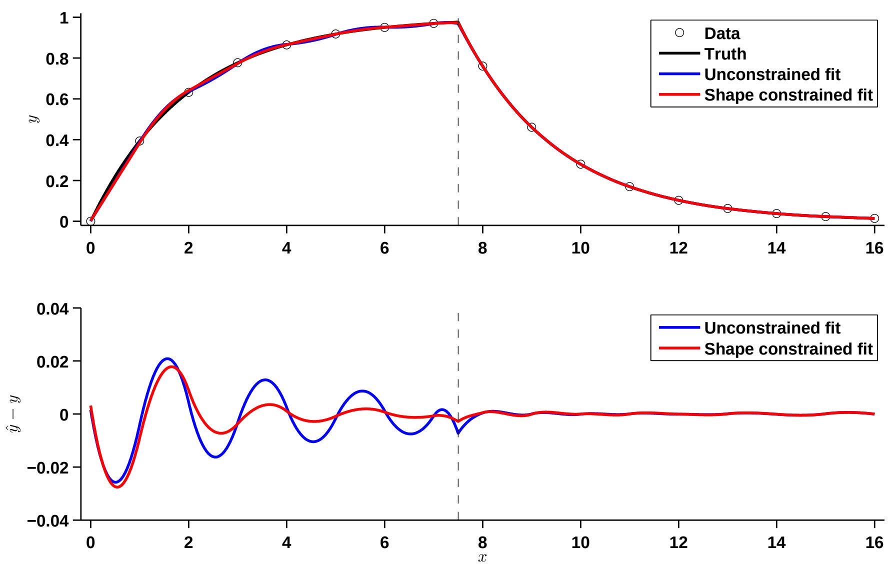

Figure 3: spline function fits.

4 Solving for θ and β

This report is continued by considering the case in which the solution to $\boldsymbol{\theta}$ is not given a priori. First the problem is sketched by means of the example. Then, the mathematical formulation to this problem is given.

4.1 Demonstration

The example above is reconsidered by evaluating the fit of the CA-shape-constrained spline function for different values of $\boldsymbol{\theta} = \theta_1 = \theta$. This means the knot with multiplicity 2 is now a variable knot. Its location and coinciding argument for the CA-transition are varied over a grid between the values $t = 0$ and $t = 16$ with steps of 0.01. The objective function is obtained by solving for β for the given value of θ. The resulting objective function value is shown as a function of θ in Fig. 4. It is relatively easy to observe that the global optimum value for θ is likely in the close neighbourhood of 7.25. However, one can also see that the objective function is non-linear in θ. While the problem appears convex in this case, this is not true in general. A global optimization strategy is therefore of interest. In addition it is required that such search strategy is deterministic if one wishes to guarantee that a global solution is found to the desired resolution in a finite number of steps. This proved possible with a branch-and-bound algorithm for the case without shape-implied discontinuities in [1]. In this work, the necessary proofs are given to make the same algorithm applicable for the more general case with shape-implied discontinuities.

4.2 Strategy

As indicated above, the values for $\boldsymbol{\theta}$ are not given. Instead, the feasible set of values for $\boldsymbol{\theta}$, Θ, is given by means of the following inequality equations:

$$\forall e = 1 \ldots n_e \quad : \quad \theta_e^L \leq \theta_e \leq \theta_e^U \tag{17}$$

$$\forall e = 1 \ldots n_e\text{-}1 \quad : \quad \epsilon_e^L \leq \epsilon_e \leq \epsilon_e^U \tag{18}$$

$$\epsilon_e \quad = \quad \theta_{e+1} - \theta_e \tag{19}$$

with definitions as follows:

- ϵ Pair-wise differences between the transition arguments
- θ_e^L Lower bound for the e^{th} transition argument

θ_e^U	Upper bound for the e^{th} transition argument
ϵ_e^L	Lower bound for the e^{th} transition argument difference
ϵ_e^U	Upper bound for the e^{th} transition argument difference

The bounds defining the above set must adhere to the following constraints:

$$\forall e = 1 \dots n_e \quad : \quad x_1 \leq \theta_e^L \leq \theta_e^U \leq x_n \tag{20}$$
$$\forall e = 1 \dots n_e - 1 \quad : \quad 0 \leq \epsilon_e^L \leq \epsilon_e^U \leq +\infty \tag{21}$$

To search for the most likely values for θ without any a priori knowledge, the feasible set Θ for θ is described by the following bounds:

$$\forall e = 1 \dots n_e \quad : \quad \theta_e^L = x_1 \tag{22}$$
$$\forall e = 1 \dots n_e \quad : \quad \theta_e^U = x_n \tag{23}$$
$$\forall e = 1 \dots n_e - 1 \quad : \quad \epsilon_e^L = 0 \tag{24}$$
$$\forall e = 1 \dots n_e - 1 \quad : \quad \epsilon_e^U = +\infty \tag{25}$$

Solving this problem deterministically is possible thanks to the branch-and-bound algorithm. To this end, one is required to apply proven bounding procedures to the objective function. The developed bounds for this task are given in the next section.

5 Bounding procedures

To enable the bounding of the objective function over any set, Θ, defined as in Eq. 17-Eq. 19, two cases must be considered. These are:

1. The set Θ is empty ($\Theta = \varnothing$)

2. The set Θ is not empty ($\Theta \neq \varnothing$)

To determine whether the set Θ is empty or not, two procedures exist. One strategy consists of applying formal methods such as solving feasibility problems [9]. A more conventional and probably intuitive strategy consists of solving the following problem, which consists of finding a solution which minimizes the following quadratic objective function over the set Θ:

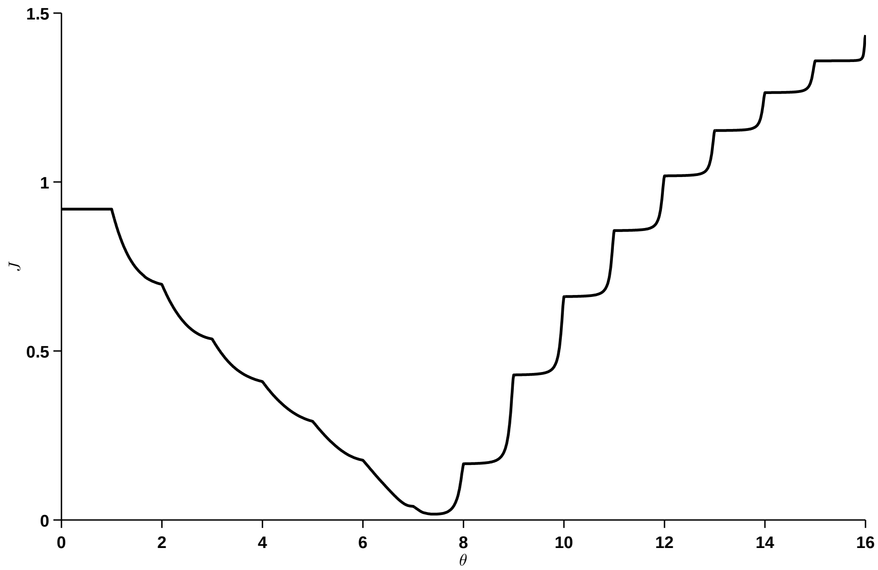

Figure 4: Objective function.

$$\min_{\boldsymbol{\theta}} \sum_{e=1}^{n_e} (\theta_e - \theta_e^L)^2 + (\theta_e - \theta_e^U)^2 \tag{26}$$

subject to:

$$\boldsymbol{\theta} \in \Theta \tag{27}$$

If no solution can be found to this problem, it follows that Θ is empty. If a feasible solution has been found one can apply it to compute an upper bound to the shape constrained spline fitting problem as will be shown below. In this case, the obtained values for $\boldsymbol{\theta}$ are further referred to as $\boldsymbol{\theta}^{QP}$. This optimization strategy is followed because of its intuitiveness and convenience.

5.1 Case 1: Θ is empty

In the first case, both lower and upper bounds to the objective function value are set to infinity:

$$\mathit{if}\, \Theta = \varnothing \quad : \quad g^L = g^U = +\infty \tag{28}$$

In this case, the proof of these bounds is rather trivial. Indeed, if no feasible solution can be found for $\boldsymbol{\theta}$, then there no solution can be found with any objective function value lower than $+\infty$. This automatically also defines the upper bound at the same value.

5.2 Case 2: Θ is not empty

In the second case, the set Θ is not empty and a feasible solution is given by $\boldsymbol{\theta}^{QP}$. In this case, bounds to the objective function can be computed as described below.

5.2.1 Upper bound to the objective function

Procedure Evaluating an upper bound in this case remains relatively trivial. In this case, one solves the problem in Eq. 12-Eq. 16 while replacing $\boldsymbol{\theta}$ by $\boldsymbol{\theta}^{QP}$. This leads to the following convex optimization problem in which $\boldsymbol{\beta}$ is optimized:

$$\min_{\boldsymbol{\beta}} g(\boldsymbol{\beta}) \quad = \quad |\boldsymbol{y} - f(\boldsymbol{\beta}, \boldsymbol{x})|^q + \sum_{j=0}^{j=d} \lambda_j \cdot \int_{x_1}^{x_n} f^j(\boldsymbol{\beta}, v)\ dv \tag{29}$$

subject to:

$$\forall k = 1 \dots n_a, \forall j = 0 \dots c_k \quad : \quad \lim_{v \to a_k^-} f^j(\boldsymbol{\beta}, v) = \lim_{v \to a_k^+} f^j(\boldsymbol{\beta}, v) \tag{30}$$

$$\forall e = 0 \dots n_e, \forall j = 0 \dots d :$$

$$b_e^L \leq v \leq b_e^U \quad \Rightarrow \quad \begin{cases} f^j(\boldsymbol{\beta}, v) \leq 0, & \textit{if } s_{e,j} = -1 \\ f^j(\boldsymbol{\beta}, v) = 0, & \textit{if } s_{e,j} = 0 \\ f^j(\boldsymbol{\beta}, v) \geq 0, & \textit{if } s_{e,j} = +1 \end{cases} \tag{31}$$

$$\boldsymbol{b}^L = [\ b_0^L \quad b_1^L \quad \dots \quad b_{n_e}^L\ ] \quad = \quad [\ x_1 \quad \theta_1^{QP} \quad \dots \quad \theta_{n_e}^{QP}\ ] \tag{32}$$

$$\boldsymbol{b}^U = [\ b_0^U \quad b_1^U \quad \dots \quad b_{n_e}^U\ ] \quad = \quad [\ \theta_1^{QP} \quad \dots \quad \theta_{n_e}^{QP} \quad x_n\ ] \tag{33}$$

Proof This optimization completes the computation of an upper bound for g. The objective function value for the computed solution is indeed an upper bound since the existence of the associated solution proves that at least one solution has a value equal or lower to this value.

5.2.2 Lower bound to the objective function

Procedure In the following, the three necessary modifications to the original problem which are necessary to obtain the lower bound are discussed.

Modification 1 To describe the computation of the lower bound, the modifications as used in [1] for the continuous case are also applied here. Concretely, this means the equations Eq. 15-Eq. 16 in the original problem are modified as follows:

$$\boldsymbol{b}^L = \boldsymbol{b}^L = [\ b_0^L \quad b_1^L \quad \ldots \quad b_{n_e}^L\ ] \quad = \quad [\ x_1 \quad \theta_1^U \quad \ldots \quad \theta_{n_e}^U\ ] \tag{34}$$

$$\boldsymbol{b}^U = \boldsymbol{b}^U = [\ b_0^U \quad b_1^U \quad \ldots \quad b_{n_e}^U\ ] \quad = \quad [\ \theta_1^L \quad \ldots \quad \theta_{n_e}^L \quad x_n\ ] \tag{35}$$

In words, the lower and upper bounds for the intervals over which shape constraints are implemented are replaced by the upper, resp. lower, bounds for the transition arguments. This modification reduces the argument intervals over which the shape constraints are active. Importantly, it holds that the shape constraints applied for the lower bound are also applied when solving with any feasible set of values for θ within the considered set:

$$\forall e = 1..n_e, \forall \theta \in \Theta : [b_e^L, b_e^U]^L \subseteq [b_e^L, b_e^U]^U \tag{36}$$

Because the applied constraints in the modified lower bounding problem are always applied for any particular choice of θ within the considered solution set, the obtained objective function following this modification, denoted here as g_1^L, is guaranteed to be lower or equal than the computed upper bound, g^U:

$$g_1^L \leq g^U \tag{37}$$

As long as no discontinuities are implied by the qualitative sequence, this modification is sufficient to obtain a provable lower bound [1]. In the more general case where some of the transitions imply the presence of a knot with multiplicity, this is not a sufficient modification to obtain a provable lower bound. Two further modifications are sufficient to achieve this. These are explained below.

Modification 2 A second modification consists of adding knots with multiplicity to the set of knots implemented for the upper bound solution.

For any transition, with index d, one denotes the corresponding index of the highest continuous derivative as c_d and θ_d^{QP} the solution for this transition argument obtained for the upper bound. Whereas c_d knots are placed in θ_d^{QP} for the upper bound, one now places $d+1$ ($d+1 \geq c_d$) knots in the same argument. This means that the spline function and all its derivatives are discontinuous in this location. As a result, the piece-wise polynomial function fitting is now completely separable since the data and polynomial coefficients on the left (right) hand side, of each discontinuity argument, θ_d^{QP}, have no influence on the polynomial coefficients for the right (left) hand side. This also implies additional degrees of freedom for the piece-wise polynomial function. In general, the number of applied constraints is either reduced or remains the same while the objective function itself remains unchanged. As a result, the resulting objective function, referred to as g_2^L, is lower or equal to the previously defined objective function value:

$$g_2^L \leq g_1^L \leq g^U \tag{38}$$

Modification 3 One more modification is necessary to obtain a provable lower bound. This modification consists of changing the objective function as follows:

$$g(\boldsymbol{\beta}) \quad = \quad \sum_i \delta_i \cdot |y_i - f(\boldsymbol{\beta}, x_i)|^q + \sum_{j=0}^{j=d} \lambda_j \cdot \int_{x_1}^{x_n} I(v) \cdot f^j(\boldsymbol{\beta}, v)\ dv \tag{39}$$

with:

$$\delta_i \quad = \quad \begin{cases} 0, & \text{if } \exists d : \theta_d^L \leq x_i \leq \theta_d^U \\ 1, & \text{otherwise} \end{cases} \tag{40}$$

$$I(v) \quad = \quad \begin{cases} 0, & \text{if } \exists d : \theta_d^L \leq v \leq \theta_d^U \\ 1, & \text{otherwise} \end{cases} \tag{41}$$

In words, the residuals corresponding to data points lying within an interval defining the potential location of any transition implying knot multiplicity are not accounted for in the objective function. In addition, the L2 penalty functions are only integrated over intervals which cannot contain a transition implying knot multiplicity. The resulting objective function value, g_3^L, is naturally lower than or equal to all previously defined objective function values:

$$g_3^L \leq g_2^L \leq g_1^L \leq g^U \tag{42}$$

The combined modifications discussed above are sufficient to obtain a provable lower bound. This is proven in the following paragraphs. The underlying principle of the proof is that adding a discontinuity in any additional feasible location does not lower the computed objective function value.

Proof To prove the lower bound, consider first that the objective function can be rewritten as a sum of terms which are associated with three contiguous and non-overlapping intervals of the argument range by using the bounds for the argument location of a discontinuity, θ_d^L and θ_d^U, as interval boundaries:

$$\begin{aligned}
\min_{\boldsymbol{\beta}} g(\boldsymbol{\beta}) \quad = \quad & \sum_{i \in S_1} \delta_i \cdot |y_i - f(\boldsymbol{\beta}, x_i)|^q & (43)\\
& + \sum_{i \in S_2} \delta_i \cdot |y_i - f(\boldsymbol{\beta}, x_i)|^q & (44)\\
& + \sum_{i \in S_3} \delta_i \cdot |y_i - f(\boldsymbol{\beta}, x_i)|^q & (45)\\
& + \sum_{j=0}^{j=d} \lambda_j \cdot \int_{x_1}^{\theta_d^L} I(v) \cdot f^j(\boldsymbol{\beta}, v)\ dv & (46)\\
& + \sum_{j=0}^{j=d} \lambda_j \cdot \int_{\theta_d^L}^{\theta_d^U} I(v) \cdot f^j(\boldsymbol{\beta}, v)\ dv & (47)\\
& + \sum_{j=0}^{j=d} \lambda_j \cdot \int_{\theta_d^U}^{x_n} I(v) \cdot f^j(\boldsymbol{\beta}, v)\ dv & (48)
\end{aligned}$$

Upon explicit evaluation of δ_i and $I(v)$ one observes that the 2$^{\text{nd}}$ and

5^{th} term are zero so that one can write:

$$\begin{aligned} \min_{\boldsymbol{\beta}} g(\boldsymbol{\beta}) &= \sum_{i\in S_1} \delta_i \cdot |y_i - f(\boldsymbol{\beta}, x_i)|^q && (49)\\ &+ \sum_{i\in S_3} \delta_i \cdot |y_i - f(\boldsymbol{\beta}, x_i)|^q && (50)\\ &+ \sum_{j=0}^{j=d} \lambda_j \cdot \int_{x_1}^{\theta_d^L} I(v)\cdot f^j(\boldsymbol{\beta}, v)\ dv && (51)\\ &+ \sum_{j=0}^{j=d} \lambda_j \cdot \int_{\theta_d^U}^{x_n} I(v)\cdot f^j(\boldsymbol{\beta}, v)\ dv && (52) \end{aligned}$$

It is now easy to verify that the objective function above cannot be lowered further by adding any knot within the interval $[\theta_d^L, \theta_d^U]$. Indeed, the fitted function as above includes two piece-wise polynomial segments, defined over the intervals $[\theta_d^L, \theta_d^{QP}]$ and $[\theta_d^{QP}, \theta_d^U]$. The polynomial coefficients of the corresponding polynomials are tied to the coefficients for the polynomials defined over intervals left, respectively right, of these intervals by means of continuity constraints. In the argument θ_d^{QP} no continuity constraints are applied. Now consider that one adds a knot in the interval $[\theta_d^L, \theta_d^{QP}]$ in the argument a. In this case, the original left-side polynomial is split into two new piece-wise polynomials with continuity constraints for the function value and the derivatives up to the $d-1^{\text{th}}$ derivative. The last (d^{th}) derivative is discontinuous. Another way to interpret this is that the original polynomial with $d+1$ coefficients is now replaced with two polynomials with a total of $2\cdot(d+1)$ coefficients and d continuity constraints between them. This indicates the net addition of a single degree of freedom. Importantly however, this added degree of freedom cannot be exploited to reduce the objective function value.

To see this, one observes that the coefficients of the polynomial terms up to degree d over $[a, \theta_d^{QP}]$ can be computed from the coefficients of the polynomial over $[\theta_d^L, a]$ thanks to existing continuity constraints. The coefficient for the $d+1^{\text{th}}$ polynomial term for the interval $[a, \theta_d^{QP}]$ remains to be chosen. Interestingly, this value can be chosen freely since the objective function is not influenced by the value of this coefficient. Any further addition of a knot in the same or other location will lead to the same effect. In summary, the further addition of any number of knots within the interval $[\theta_d^L, \theta_d^{QP}]$ adds degrees of freedom to the fitted function which cannot be used to improve the objective function because this objective function is not sensitive to the added parameters. Furthermore, the set of applied constraints does not change when adding such additional knots. Similarly, the addition of any number of knots within the interval $[\theta_d^{QP}, \theta_d^U]$ cannot be used to lower the computed objective function value.

In the above paragraphs, three modifications were shown to lead to a provable lower bound. The modifications are considered sufficient conditions to compute the lower bound. It is not clear whether these conditions are also necessary, in contrast to the study in [1].

6 Conclusions

This technical report describes and proves bounding procedures which are sufficient to permit a generalized form of shape constrained spline fitting, namely when the shape constraints imply knots of multiplicity in the spline function. Most interestingly, it appears that the lower bound, while applicable, is not an efficient one. This suggests that the applied modifications to the optimization problem are possibly sufficient but not necessary to obtain a provable lower bound. Whether this is the case and whether or how a more efficient lower bounding procedure is unclear at the time of writing of this document.

Acknowledgements

All results were obtained by joint use of Matlab [10] and the Functional Data Analysis software package accompanying the book Ramsay and Silverman [11].

References

[1] V. Venkatasubramanian, R. Rengaswamy, and S. N. Kavuri. A review of process fault detection and diagnosis - Part II: Qualitative models and search strategies. *Comput. Chem. Eng.*, 27:313–326, 2003.

[2] K. Villez, C. Rosén, F. Anctil, C. Duchesne, and P. A. Vanrolleghem. Qualitative representation of trends (QRT): Extended method for identi-

fication of consecutive inflection points. *Comp. Chem. Eng.*, 48:187–199, 2012.

[3] K. Villez, R. Rengaswamy, and V. Venkatasubramanian. Generalized shape constrained spline fitting for qualitative analysis of trends. *Comp. Chem. Eng.*, 58:116–134, 2013.

[4] Y. Nesterov. *High Performance Optimization, Applied Optimization*, volume 33, chapter Squared functional systems and optimization problems, pages 405–440. Kluwer Academic Publishers, 2000.

[5] D. Papp. *Optimization models for shape-constrained function estimation problems involving nonnegative polynomials and their restrictions.* PhD thesis, Rutgers University, 2011.

[6] M. Grant and S. Boyd. CVX: Matlab software for disciplined convex programming, version 1.21., 2011. URL `http://cvxr.com/cvx`.

[7] E. D. Andersen and K. D. Andersen. The MOSEK interior point optimizer for linear programming: an implementation of the homogeneous algorithm. *High performance optimization*, 33:197–232, 2000.

[8] MOSEK ApS. *MOSEK Optimization Software for MATLAB, Version 6.0.* Available from http://www.mosek.com/, 2012.

[9] S. Boyd and L. Vandenberghe. *Convex optimization.* Cambridge University Press, 2009.

[10] The MathWorks Inc. *Matlab, version 7.10.0 (R2010a).* Natick, Massachusetts, 2010.

[11] J. O. Ramsay and B. W. Silverman. *Applied Functional Data Analysis: Methods and Case Studies.* Springer-Verlag, 2002.